

# Chapter 5

## The direct calculation approach

It is the aim of this chapter to present the process for generating the theoretical readout signal from the Type 1 reflectance, single detector and differential detector MO scanning microscopes by implementing the analysis presented in chapters 3 and 4 in computer code. The so-called direct calculation approach <sup>[59]</sup> involves the formulation of the optical field as it propagates through the optical system to the detector, as the sample is scanned beneath the focused spot. A similar approach was applied by Jipson and Williams <sup>[67]</sup> for developing a two-dimensional model of the theoretical readout process in reflectance-based optical disc systems. Here we are concerned both with reflectance and MO imaging systems.

The optical field distribution is represented by a two-dimensional matrix, the complex elements of which correspond to sample points across the optical field. The aperture pupil functions are represented by similar two-dimensional matrices where the elements in the matrix correspond to the transmission properties of the pupil at sample points across its surface. The Fourier transform operation is performed using the Fast Fourier Transform (FFT) algorithm <sup>[42,68]</sup>.

The signal generation process, using the direct calculation approach, is relatively straight forward to implement computationally. However, the direct calculation approach is also computationally demanding if a high resolution signal is required, due to the large number of sample points required to represent accurately the optical field, aperture pupil functions and the sample characteristics. Since the resolution of the scanning microscope is determined primarily by the size and shape of the focused spot, then to obtain a high resolution output signal the focused field distribution needs to be represented by as many sample points as possible. The relationship between the resolution of the matrix containing the aperture pupil function and the matrix

containing the focused spot is determined by Fourier transform and scalar diffraction theory analysis and is described below.

The focused spot is given by the two-dimensional Fourier transform of the aperture pupil function, eq. (2.9). Considering the one-dimensional case initially, the Fourier transform may be expressed in the conventional form <sup>[4,7,42]</sup>

$$g(m) = \int_{-\infty}^{\infty} f(x) \exp\{-2\mathbf{p}jxm\} dx \quad (5.1)$$

where  $x$  represents the spatial domain and  $m$  represents the spatial frequency domain. Using scalar diffraction theory the one-dimensional focused spot is given by

$$\Psi\left(\frac{m}{\mathbf{1}f}\right) = \int_{-\infty}^{\infty} p(x) \exp\left\{-\frac{2\mathbf{p}j}{\mathbf{1}f} xm\right\} dx \quad (5.2)$$

where  $p(x)$  represents the aperture pupil function, for a clear aperture of width  $2a$ , and  $f$  is the focal length of the lens. Comparing eq. (5.2) and eq. (5.1) it can be seen that the components within the focal plane  $\{m\}$  are scaled by  $1/\mathbf{1}f$ , and that the units in both the aperture pupil plane  $\{x\}$  and the focal plane  $\{m\}$  are in terms of length.

Using the properties of the discrete Fourier transform, the spatial resolution in the focal plane,  $\Delta m$ , is given by

$$\frac{\Delta m}{\mathbf{1}f} = \frac{1}{m\dim\Delta x} \quad (5.3)$$

where  $m\dim$  represents the size of the matrix (vector) containing the aperture pupil function, and  $\Delta x$  represents the spatial resolution in the aperture pupil plane. If the size of the matrix containing the aperture pupil function,  $m\dim$ , is a function of the width of the aperture, i.e.

$$m\dim\Delta x = ca \quad (5.4)$$

where  $c$  is a multiplication factor, then substituting eq. (5.4) into eq. (5.3) gives

$$\frac{\Delta m}{\mathbf{1}f} = \frac{1}{ca} \cdot \quad (5.5)$$

Assuming the numerical aperture of the lens,  $NA$ , is approximately

$$NA \approx \frac{a}{f} \quad (5.6)$$

then

$$\Delta m = \frac{I}{cNA}. \quad (5.7)$$

Hence, to produce for example a focused spot which has a resolution of  $0.05I/NA$ , i.e. each element of the matrix represents  $0.05I/NA$ , then using eq. (5.7), it can be seen that  $c = 20$ . If the size of the matrix,  $mdim$ , is 512 elements, then the width or the aperture pupil function, given by  $2a$ , is represented by approximately 51 elements within that matrix. Therefore, to produce a high resolution focused spot whilst maintaining a high resolution aperture pupil function is extremely difficult, and requires the application of very large matrices,  $> 512$  elements. This increases the size of the calculation considerably, and hence the calculation time. Hence, it is for this reason that the direct calculation approach is restricted in this thesis to imaging in the Type 1 system and not confocal systems where the imaging process is much more complicated. The resolution of the object is determined by the resolution of the focused spot.

## 5.1 Modelling the Type 1 reflectance scanning microscope

In the following section the direct calculation approach will be applied to imaging in the Type 1 reflectance scanning microscope.

### Computational procedure

The computational procedure for calculating the response follows directly from the analysis presented in sec. 3.2, and involves the evaluation of eq. (3.1) - eq. (3.10) in computer code. The direct calculation approach can be applied to generate images of both one-dimensional and two-dimensional, simple or complex (i.e. amplitude and phase), reflectance objects. In the current analysis the two-dimensional imaging process will be described in detail.

In the following analysis the aperture pupil functions are represented by two-dimensional matrices of dimensions  $adim \times adim$ , the reflectance object is represented by a square matrix of dimensions  $odim \times odim$ , and the focused field distribution is represented by a two-dimensional matrix of dimensions  $fdim \times fdim$ , where  $fdim \ll odim$ . Thus, the resulting two-dimensional image is represented by a two-dimensional matrix of dimensions  $odim-fdim \times odim-fdim$ .

Figure 5.1 illustrates the direct calculation approach for generating the image of a two-dimensional reflectance sample and is described in detail as follows.

- Step 1*
- Generate a matrix containing the objective aperture pupil function,  $p_o$ , which is of dimensions  $adim \times adim$ .
  - Generate a matrix containing the collector aperture pupil function,  $p_c$ , which is of dimensions  $adim \times adim$ .
  - Generate a matrix of containing the incident field distribution,  $\mathbf{y}_1$ , which is of dimensions  $adim \times adim$ .
  - Generate a matrix representing the reflectance characteristics of the two-dimensional sample,  $r$ , which is of dimensions  $odim \times odim$ . The resolution of the object is determined by the desired spot resolution,  $\Delta m$ .

The aperture pupil functions are centred in a larger two-dimensional matrix of dimensions  $mdim \times mdim$ . If  $adim/2=a$ , then using the analysis developed in the previous section the resolution of the focused field distribution,  $\Delta m$ , can be easily calculated.

- Step 2* Calculate the matrix,  $\mathbf{y}_2$ , representing the field distribution immediately after the objective lens by array multiplying the incident field distribution matrix,  $\mathbf{y}_1$ , and the objective aperture pupil function matrix,  $p_o$ .  $\mathbf{y}_2$  is a two-dimensional matrix of dimensions  $mdim \times mdim$ .
- Step 3* Take the two-dimensional fast Fourier transform of the field distribution matrix  $\mathbf{y}_2$  to calculate the matrix,  $\mathbf{y}_3$ , representing the field distribution at

the scan position on the surface of the reflectance sample. The focused field distribution is then represented by a two-dimensional matrix of dimensions  $mdim \times mdim$ . However, the majority of the matrix elements are equal to zero, hence, the field may be represented by a smaller central area of the matrix of dimensions  $fdim \times fdim$ , this will help speed up the computational procedure.  $\mathbf{y}_3'$  represents the smaller matrix containing the focused field distribution and is of dimensions  $fdim, \times fdim$ .

*Step 4* Calculate the matrix,  $\mathbf{y}_4$ , representing the field distribution after interaction with the sample, by array multiplying the field distribution matrix,  $\mathbf{y}_3'$ , representing the focused field distribution and the matrix representing the reflectance properties of the sample,  $r$ , about the scan position on the current scan line.  $\mathbf{y}_4$  is a two-dimensional matrix of dimensions  $mdim \times mdim$ .

*Step 5* Take the two-dimensional fast Fourier transform of the field matrix  $\mathbf{y}_4'$  to calculate the matrix,  $\mathbf{y}_5$ , representing the field distribution in the plane of the collector lens.

*Step 6* Calculate the matrix,  $\mathbf{y}_6$ , representing the field distribution immediately after the collector lens by array multiplying the field distribution matrix  $\mathbf{y}_5$  and the collector aperture pupil function matrix,  $p_c$ .  $\mathbf{y}_6$  represents the field distribution incident on the photo-detector.

*Step 7* The signal from the photo-detector,  $I_{j,l}$ , for the current scan position  $(j, l)$ , is calculated by taking the sum of the square magnitude of each element of the field distribution matrix,  $\mathbf{y}_6$ , representing the field distribution incident on the photo-detector.

*Step 8* Repeat *Steps 4 - 7* for each scan position along the sample to generate the response along the current scan line.

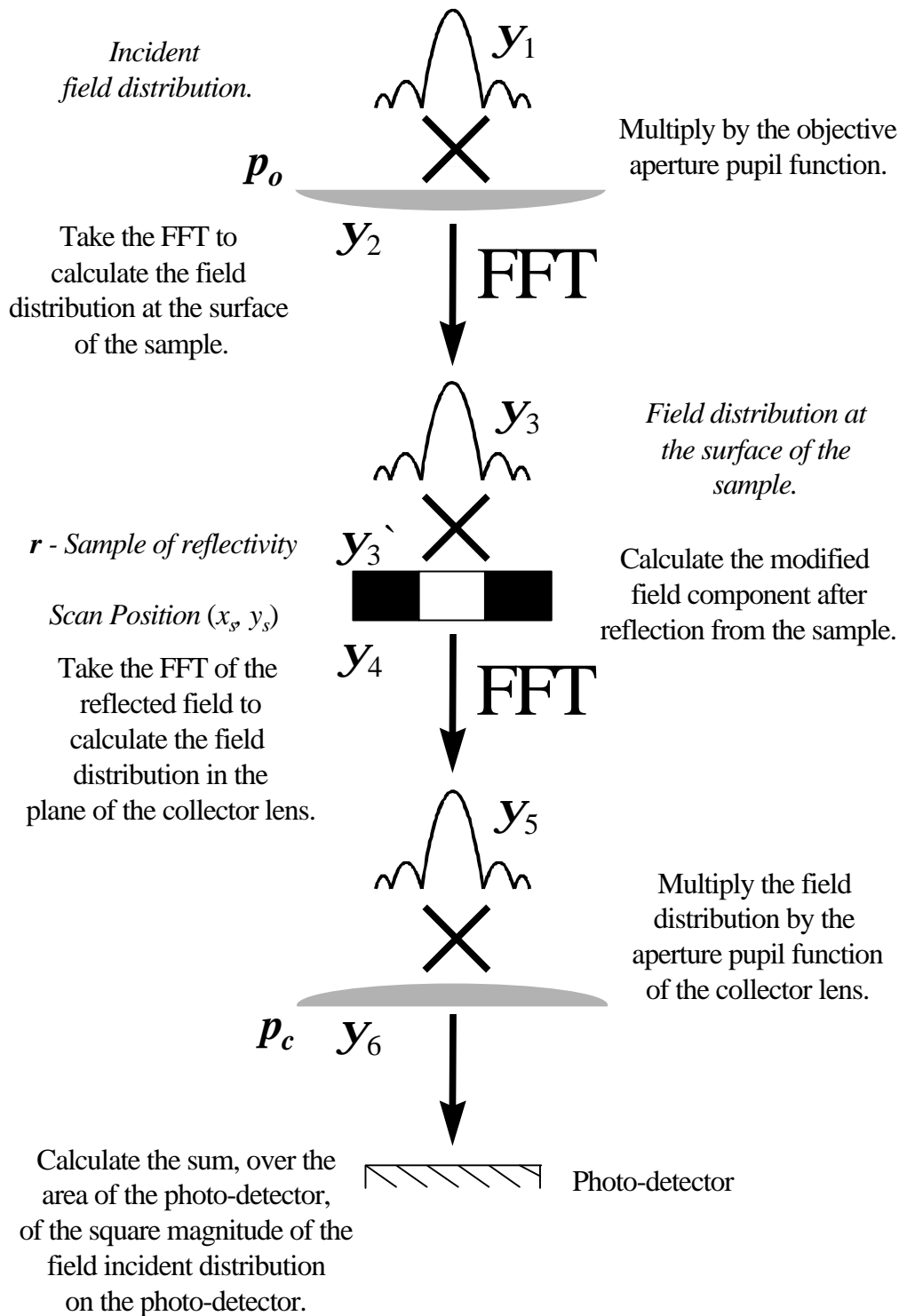


**Figure 5.1** : The signal generation process in the Type 1 reflectance scanning microscope generated using the direct calculation approach.

*Step 9* Centre the focused field distribution on the next scan line and repeat *Steps 4-8* for each scan line to generate a two-dimensional matrix,  $I$ , representing the image of the two-dimensional reflectance sample generated by the Type 1 reflectance scanning microscope.

The process described is implemented in computer code, the algorithm for which is described in the following section.

### The direct calculation algorithm

The following algorithm, written in pseudocode (see Appendix B), illustrates the computational procedure for calculating the image of a two-dimensional object using the direct calculation approach for modelling the response of the Type 1 reflectance scanning microscope.

*Step 1.* Input data. Matrix containing the objective aperture pupil function -  $p_o$ , of dimensions  $adim \times adim$ .  
 Matrix containing the collector aperture pupil function -  $p_c$ , of dimensions  $adim \times adim$ .  
 Matrix containing the incident field distribution -  $\mathbf{y}_1$ , of dimensions  $adim \times adim$ .  
 Matrix containing the sample reflectance characteristics -  $r$ , of dimensions  $odim \times odim$  (two-dimensional reflectance object).

Output data. Matrix representing the image generated by the Type 1 reflectance scanning microscope -  $I$ , of dimensions  $odim-fdim \times odim-fdim$ .

*Step 2* FOR  $y = 1, 2, \dots, adim$   
 FOR  $x = 1, 2, \dots, adim$   
 Set  $\mathbf{y}_2(y + (mdim - adim) / 2, x + (mdim - adim) / 2) = \mathbf{y}_1(y, x) \times p_o(y, x);$   
 END;  
 END.

*Step 3* Set  $\mathbf{y}_3 = \text{Fast Fourier Transform } (\mathbf{y}_2);$ <sup>#1</sup>  
 FOR  $y = 1, 2, \dots, fdim$   
 FOR  $x = 1, 2, \dots, fdim$   
 Set  $\mathbf{y}_3'(y, x) = \mathbf{y}_3(y + (mdim - fdim) / 2, x + (mdim - fdim) / 2);$

```

        END;
    END;
    Set  $i = 0$ ;          ( $i$  represents the scan position along the
    Set  $j = 0$ .          current scan line  $j$ )
Step 4  FOR  $y = 1, 2, \dots, fdim$ 
        FOR  $x = 1, 2, \dots, fdim$ 
            Set  $\mathbf{y}_4(y + (mdim - fdim) / 2, x + (mdim - fdim) / 2) =$ 
                 $\mathbf{y}_3'(y, x) \times r((y + j), (x + i));$ 
        END;
    END;
Step 5  Set  $\mathbf{y}_5 =$  Fast Fourier Transform ( $\mathbf{y}_4$ ). #1
Step 6  FOR  $y = 1, 2, \dots, adim$ 
        FOR  $x = 1, 2, \dots, adim$ 
            Set  $\mathbf{y}_6(y + (mdim - adim) / 2, x + (mdim - adim) / 2) =$ 
                 $\mathbf{y}_5(y + (mdim - adim) / 2, x + (mdim - adim) / 2) \times p_c(y, x);$ 
        END;
    END;
Step 7  Set  $I(j, i) = \sum_{y=1}^{y=mdim} \sum_{x=1}^{x=mdim} |\mathbf{y}_6(y, x)|^2$ ;
        Set  $i = i + 1$ .      (Increment the scan position)
Step 8  WHILE  $i < (odim - fdim)$  DO Steps 4-7.
Step 9  Set  $j = j + 1$ ;      (Increment the scan line)
        WHILE  $j < (odim - fdim)$  DO Steps 4-8;
    STOP.

```

#1 Fast Fourier Transform algorithm is described in reference 68.

The response to a simple one-dimensional object may be generated using a similar algorithm to that presented above. However, in the one-dimensional case the rows of the two-dimensional matrix represent the properties of the one-dimensional reflectance object and the response is generated along a single scan line.

### Step response

The code just described was used to generate the image for the simple one-dimensional step object shown in Fig. 5.2. The step is in reflectance from 0% (no reflectance) to 100% (total reflectance); the scan direction is in  $x$ . The result is illustrated in Fig. 5.3, for clear, aberration free, circular apertures of equal diameter under both uniform and Gaussian ( $w_{e^{-2}} = a/2$ ) incident illumination.



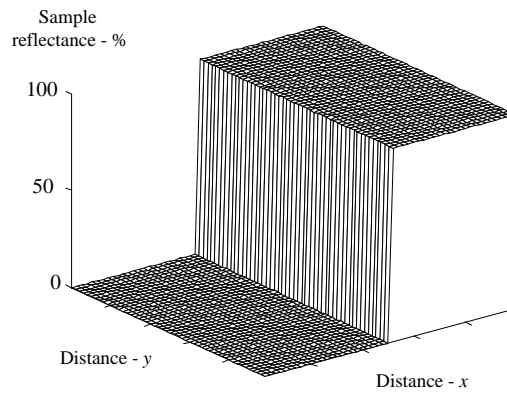


**Figure 5.2 :** *The theoretical one-dimensional step in reflectance used to generate the step response illustrated in Figure 5.3; the scan direction is in  $x$ .*

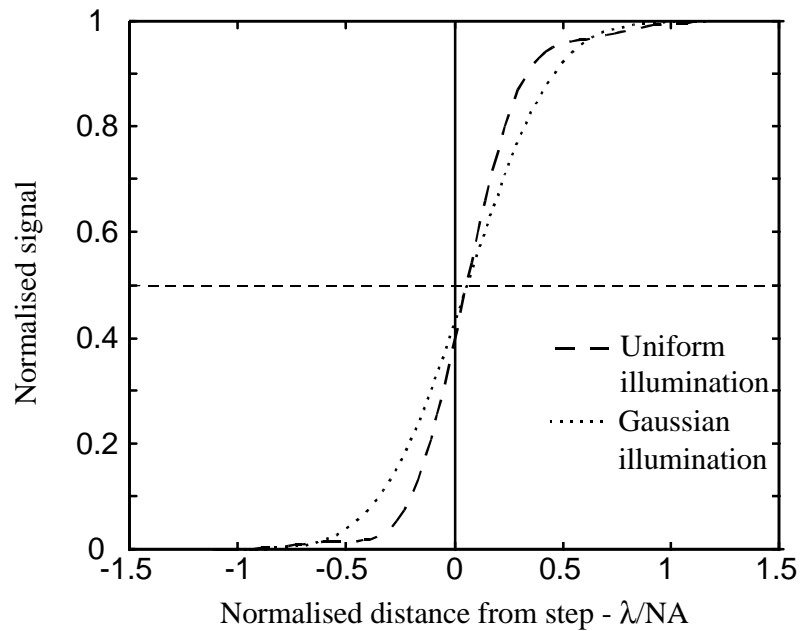


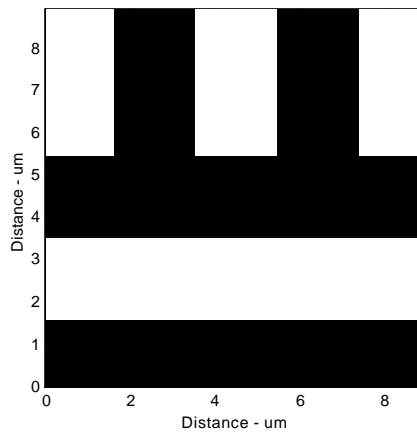
**Figure 5.3 :** *The step response of the Type 1 reflectance scanning microscope for the one-dimensional step illustrated in Fig 5.2, for clear, aberration free, circular apertures of equal diameter under uniform (bold dashed line) and Gaussian ( $w_{e-2} = a/2$ ) (dotted line) incident illumination.*

As expected from discussions in chapter 2, the response under uniform illumination is sharper than that under Gaussian illumination. However, under uniform illumination the Airy disc focused spot gives rise to side lobes and these translate to ‘wiggles’ at the extremes of the step. It should be noted that a shift of the midpoint in the response to an edge is evident in the readout signal, which for a coherence ratio of  $g = 1$  is

approximately  $0.05\lambda/NA$ , this corresponds to  $0.05\mu\text{m}$  for a wavelength of  $514\text{nm}$  and objective lens NA of  $0.5$ .

### Two-dimensional imaging

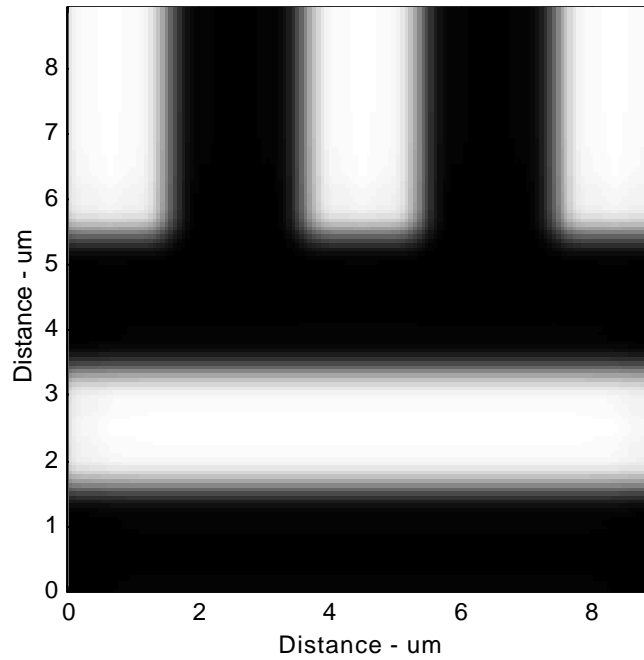
Figure 5.4 illustrates a two-dimensional reflectance object which represents a commercially available resolution test target. The lines are of width  $2\mu\text{m}$ , length  $10\mu\text{m}$  and spacing  $2\mu\text{m}$ . Such a test target is often used to assess the imaging characteristics of an optical system and to determine its MTF.



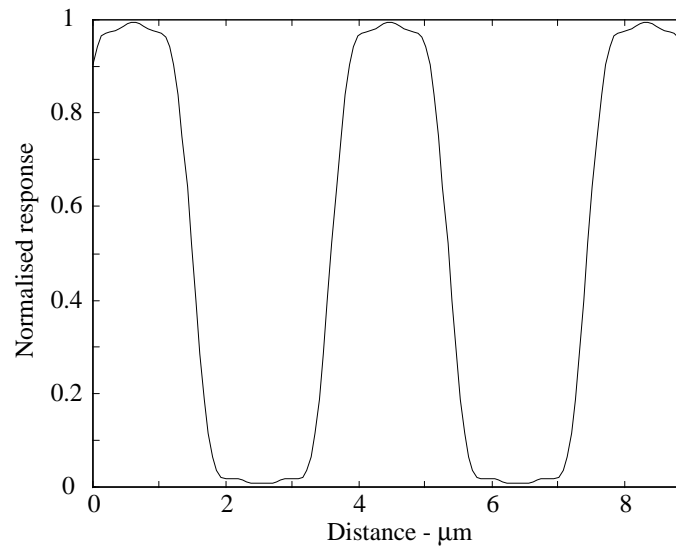
**Figure 5.4** : *Two-dimensional reflectance object representing a commercial optical test target. Black corresponds to non reflective areas and white corresponds to reflective areas. The sample resolution is  $0.0625\lambda/NA$  which corresponds to  $0.06425\text{mm}$  for a wavelength of  $514\text{nm}$  and objective NA of  $0.5$ .*

Figure 5.5 illustrates the image of the simple test target of Fig. 5.4 for clear, aberration free, circular apertures under uniform incident illumination, generated using the direct calculation algorithm presented previously.

Figure 5.6 illustrates a line plot along the bars at the top of Fig. 5.5, illustrating the quantitative nature of the image.



**Figure 5.5 :** *Image of the two-dimensional test target illustrated in Fig. 5.4 generated using the direct calculation approach, for clear, aberration free, circular apertures of equal diameter, under uniform illumination.*



**Figure 5.6 :** *Plot along the bars at the top of Fig. 5.6.*

An example of the advantage of this modelling approach is the ability to investigate the effects of cross-talk in optical disc systems, and the effects of tracking error, which is illustrated for the MO case in secs. 5.2 and 5.3.

## 5.2 Modelling the single detector MO scanning microscope

In the following section the direct calculation approach is applied to imaging in the Type 1 single detector MO scanning microscope. The analysis follows directly from that presented for the Type reflectance system, described in sec. 5.1. However, in the magneto-optic scanning microscope the propagation of orthogonal field components must be traced after interaction with the MO sample. Hence, the computational procedure involves the generation of two matrices to represent the orthogonal,  $x$  and  $y$ , field components after interaction with the MO sample.

### Computational procedure

The computational procedure for calculating the two-dimensional response follows directly from the analysis presented in sec. 4.1.1, and involves the evaluation of eq. (4.1) to eq. (4.11) in computer code. The matrix dimensions and signal resolution are determined using the analysis described previously.

Figure 5.7 illustrates the direct calculation approach for generating the response to a one-dimensional MO sample, and is described in detail as follows.

The subscripts  $x$  and  $y$  indicate the corresponding  $x$  and  $y$  orthogonal field distributions.

- Step 1*
- Generate a matrix containing the objective aperture pupil function,  $p_o$ , which is of dimensions  $dim \times adim$ .
  - Generate a matrix containing the collector aperture pupil function,  $p_c$ , which is of dimensions  $adim \times adim$ .
  - Generate a matrix of containing the incident field distribution,  $\mathbf{y}_{1_x}$ , which is of dimensions  $adim \times adim$ .
  - Generate a matrix representing the reflectance characteristics of the sample,  $r$ , which is of dimensions  $odim \times odim$ .
  - Generate a matrix representing the Kerr rotation characteristics of the

sample,  $k$ , which is of dimensions  $odim \times odim$ .

- Generate a matrix representing the phase characteristics of the sample,  $\mathbf{f}$ , which is of dimensions  $odim \times odim$ .

The aperture pupil functions are centred in a larger two-dimensional matrix of dimensions  $mdim \times mdim$ . If  $adim/2=a$ , then using the analysis developed previously the resolution of the focused field distribution,  $\Delta m$ , can be easily calculated.

*Step 2* Calculate the matrix,  $\mathbf{y}_{2_x}$ , representing the field distribution immediately after the objective lens by array multiplying the incident field distribution matrix,  $\mathbf{y}_{1_x}$ , and the objective aperture pupil function matrix,  $p_o$ .  $\mathbf{y}_{2_x}$  is a two-dimensional matrix of dimensions  $mdim \times mdim$ .

*Step 3* Take the two-dimensional fast Fourier transform of the field distribution matrix  $\mathbf{y}_{2_x}$  to calculate the matrix,  $\mathbf{y}_{3_x}$ , representing the field distribution at the scan position on the surface of the reflectance sample. As previously generate a matrix  $\mathbf{y}'_{3_x}$  representing the focused field distribution which is of dimensions  $fdim \times fdim$ .

*Step 4* Calculate the matrices,  $\mathbf{y}_{4_x}$  and  $\mathbf{y}_{4_y}$ , representing the orthogonal field components after interaction with the MO sample.

- The  $x$  field component,  $\mathbf{y}_{4_x}$ , is calculated by array multiplying the field distribution matrix  $\mathbf{y}_{3_x}$  representing the focused field distribution and the matrix,  $r$ , representing the reflectance properties of the sample, about the scan position.
- The  $y$  field component,  $\mathbf{y}_{4_y}$ , is calculated by array multiplying the field distribution matrix  $\mathbf{y}_{3_x}$  representing the focused field distribution and the matrices  $r$ ,  $k$  and  $\mathbf{f}$ , representing the reflectance characteristics, the Kerr rotation characteristics and phase characteristics of the sample,

about the scan position.  $\mathbf{y}_{4_x}$  and  $\mathbf{y}_{4_y}$  are two-dimensional matrices of dimensions  $mdim \times mdim$ .

- Step 5* Take the two-dimensional fast Fourier transform of the field matrices  $\mathbf{y}_{4_x}$  and  $\mathbf{y}_{4_y}$  to calculate the corresponding matrices,  $\mathbf{y}_{5_x}$  and  $\mathbf{y}_{5_y}$ , representing the orthogonal field distributions in the plane of the collector lens.
- Step 6* Calculate the matrices,  $\mathbf{y}_{6_x}$  and  $\mathbf{y}_{6_y}$ , representing the orthogonal field distributions immediately after the collector lens by array multiplying the orthogonal field distribution matrices,  $\mathbf{y}_{5_x}$  and  $\mathbf{y}_{5_y}$ , and the collector aperture pupil function matrix,  $p_c$ .
- Step 7* Calculate the matrix,  $\mathbf{y}_7$ , representing the field distribution immediately after the analyser by calculating the field distribution along the transmission axis of the analyser, which is aligned at an angle  $\mathbf{b}$  to the plane of the incident polarisation,  $\mathbf{y}_{1_x}$ , using eq. (4.6).  $\mathbf{y}_7$  represents the field distribution incident on the photo-detector.
- Step 8* The signal from the photo-detector,  $I_{j,i}$ , for the current scan position,  $(j, i)$ , is calculated by taking the sum of the square magnitude of each element of the field distribution matrix,  $\mathbf{y}_7$ , representing the field distribution incident on the photo-detector.
- Step 9* Repeat *Steps 4 - 8* for each scan position along the sample to generate the response along the current scan line.
- Step 10* Centre the focused field distribution on the next scan line and repeat *Steps 4-9* for each scan line to generate a two dimensional matrix,  $I$ , representing the image of the two-dimensional object generated by the Type 1 single detector MO scanning microscope.

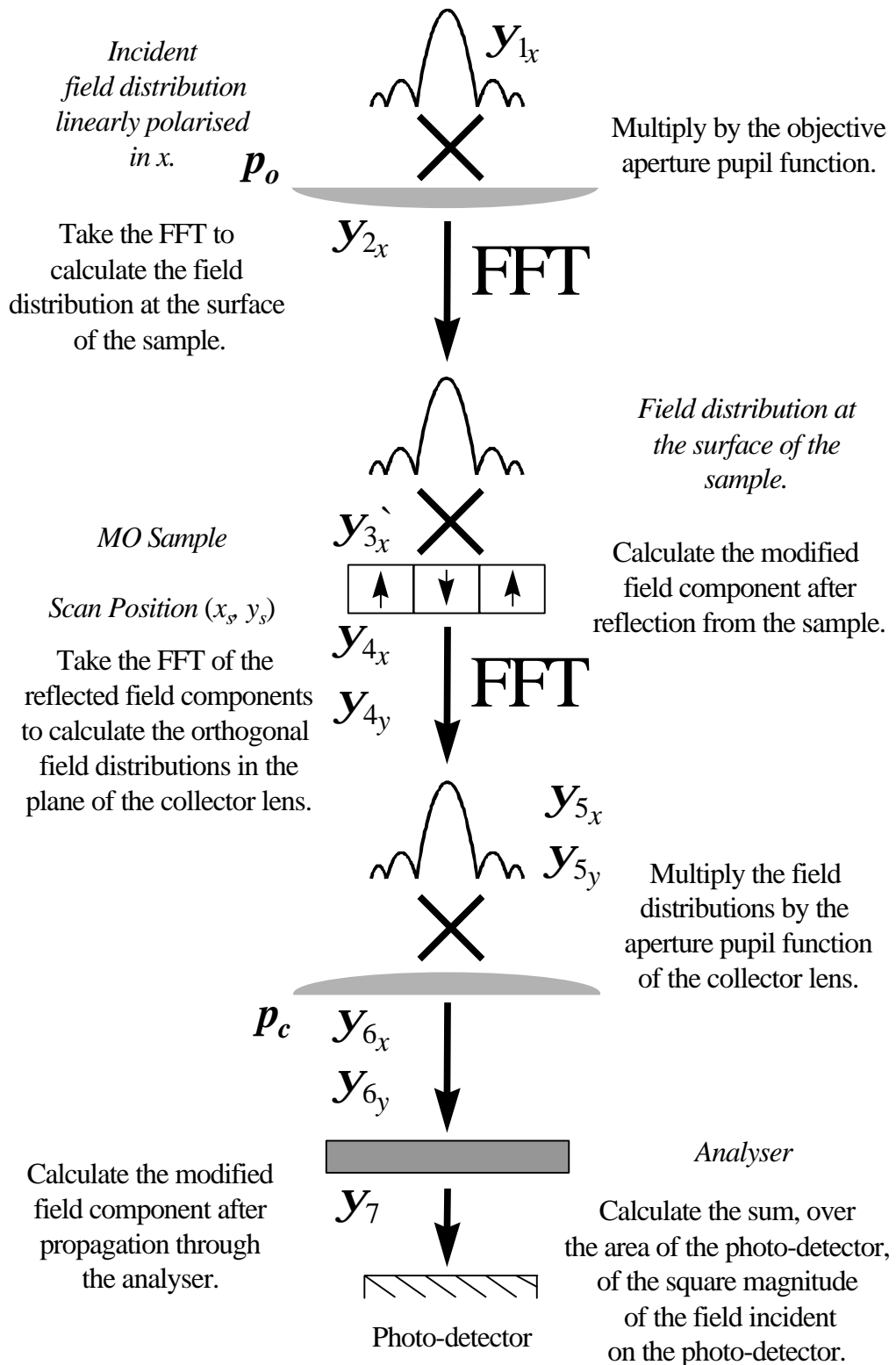


**Figure 5.7 :** The signal generation process in the Type 1 single detector MO system generated using the direct calculation approach.







## Step response

Figure 5.8 illustrates a simple one-dimensional object in  $x$ , that is infinite in extent in  $y$ , and which represents a step in Kerr rotation from  $-1^\circ$  to  $+1^\circ$ ; the scan direction is in  $x$ . The MO object illustrated in Fig. 5.8 was used to generate the step response illustrated in Fig. 5.9, using the algorithm presented above.

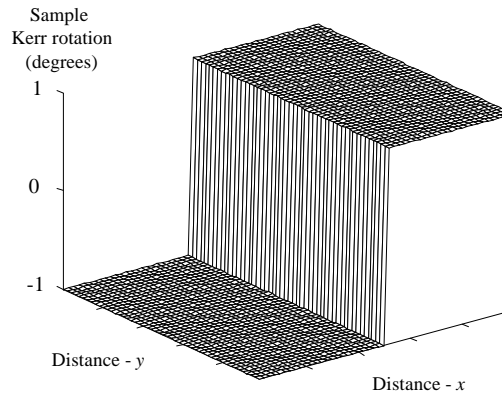


**Figure 5.8 :** *The theoretical one-dimensional step in Kerr rotation, for an MO sample of uniform reflectance (equal to one) and of zero phase, used to generate the step response illustrated in Figure 5.9.*

The responses in Fig 5.9 were generated using clear, aberration free, circular apertures of equal diameter under both uniform and Gaussian ( $w_{e^{-2}} = a/2$ ) incident illumination, for an analyser angle of  $90^\circ$  to the plane of incident polarisation (extinction position).

Figure 5.9 illustrates that the single detector MO scanning microscope detects the change in the magnitude of the Kerr rotation. However, it can only produce a unipolar signal, due to the single detector configuration, and so is unable to distinguish the polarity of rotation. The result of Fig. 5.9 indicates that the optimally aligned Type 1 single detector MO channel ( $b=90^\circ$ ) is a phase contrast detection system, where the change in rotation is measured from the photo-detector. It should be noted that it is common to operate the Type 1 single detection MO channel with the analyser aligned at  $\approx 8^\circ$  to the extinction position to maximise the signal-to-noise ratio <sup>[20]</sup>.

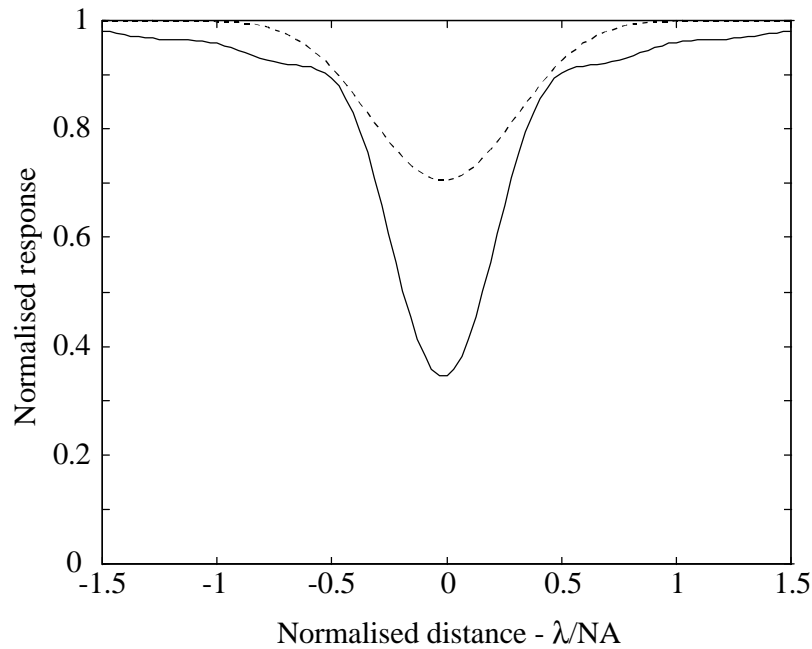


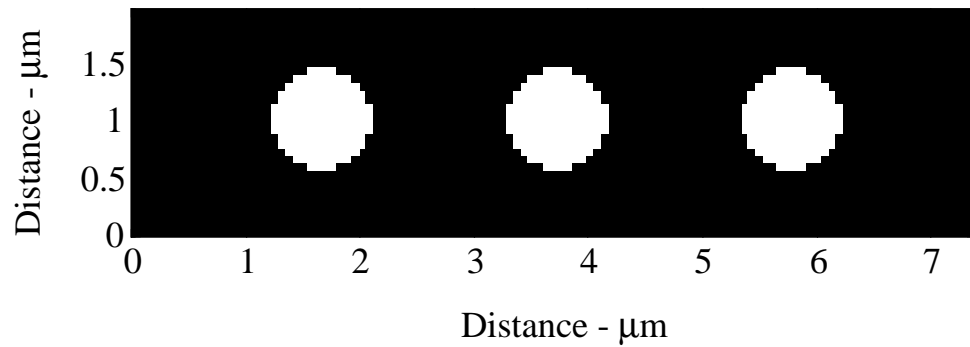
**Figure 5.9 :** *The step response of the Type 1 single detector MO system for the one-dimensional step illustrated in Fig. 5.6, for clear, aberration free, circular apertures of equal diameter under uniform (solid line) and Gaussian ( $w_{e^{-2}} = a/2$ ) (dashed line) incident illumination, for an analyser orientation of  $\mathbf{b}=90^\circ$  to the angle of incident polarisation, generated using the direct calculation approach.*

### Two-dimensional imaging

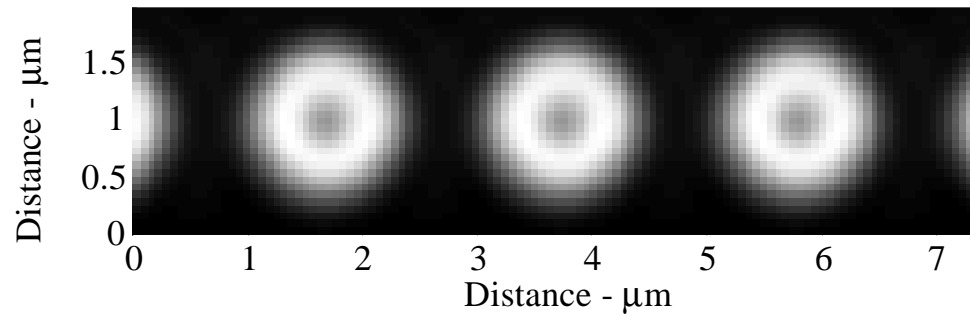
In the following section the imaging of two-dimensional MO objects using the direct calculation approach for modelling the response of the Type 1 single detector MO scanning microscope is presented.

Figure 5.10 illustrates a MO object comprising a series of circular bits, of diameter  $1\mu\text{m}$  and spacing  $1\mu\text{m}$ . The Kerr rotation inside the bits is  $+1^\circ$  and outside  $-1^\circ$ .

Figure 5.11 illustrates the image of the bits of Fig 5.10 The image was generated with clear, aberration free, circular apertures of equal diameter, under uniform incident illumination.



**Figure 5.10 :** *Two-dimensional MO object comprising a track of circular MO bits of diameter 1 $\mu\text{m}$  and spacing 1 $\mu\text{m}$ . The Kerr rotation of the bits (white areas) is  $+1^\circ$ , and elsewhere (black areas)  $-1^\circ$ .*



**Figure 5.11 :** *Image of MO bits illustrated in Fig 5.10, using the Type 1 single detector MO scanning microscope generated using the direct calculation approach.*

Figure 5.12 illustrates the effects on the signal amplitude when scanning the focused beam along a track at varying distances from the centre of the track. Such a process can be used to investigate the effects of tracking error and cross-talk in optical disc systems.

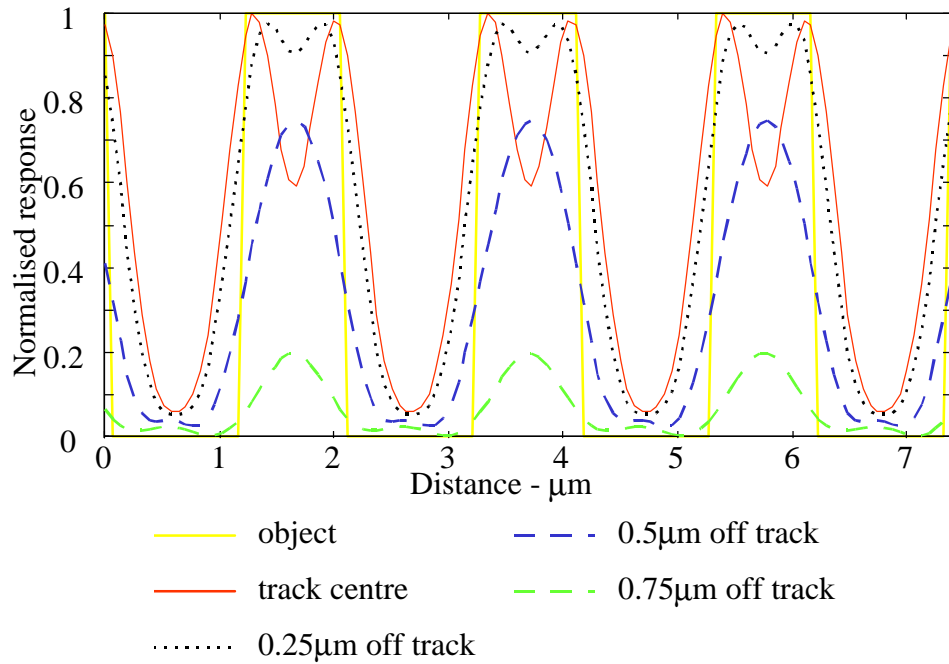


**Figure 5.12 :** *Plots of signal profile at varying distances from the track centre for the two-dimensional image illustrated in Fig. 5.11*

### 5.3 Modelling the differential detector MO scanning microscope

In the following section the direct calculation approach is applied to imaging in the Type 1 differential detector MO scanning microscope. The analysis follows directly from that presented for the Type 1 single detector MO system, described in sec. 5.2.

#### Computational procedure

The computational procedure for calculating the response follows directly from the analysis presented in sec. 4.1.1 and sec. 4.2.1, and involves the evaluation of eq. (4.1) to eq. (4.5) and eq. (4.32) to eq. (4.35) in computer code. The matrix dimensions and signal resolution are determined using the analysis described previously.

Figure 5.13 illustrates the direct calculation approach for generating the response to a two-dimensional MO sample, and is described in detail as follows.

The subscripts  $x$  and  $y$  indicate the corresponding  $x$  and  $y$  orthogonal field distributions.

*Steps 1 to 6* are as detailed for the single detector case.

*Step 7* Calculate the field matrices,  $\mathbf{y}_{7_x}$  and  $\mathbf{y}_{7_y}$ , representing the modified orthogonal field distributions immediately after the half wave plate, which has its fast axis aligned at an angle  $\mathbf{q}$  to the plane of the incident polarisation,  $\mathbf{y}_{1_x}$ , using eq. (4.33).

*Step 8* Calculate the signals from each of the two photo-detectors.

- The signal from the photo-detector 1,  $I_{Det1}$ , for the current scan position,  $(j, i)$ , is calculated by taking the sum, of the square magnitude, of each element of the field distribution matrix,  $\mathbf{y}_{7_x}$ , representing the  $x$  field distribution incident on the photo-detector.
- The signal from the photo-detector 2,  $I_{Det2}$ , for the current scan position,  $(j, i)$ , is calculated by taking the sum, of the square magnitude, of each element of the field distribution matrix,  $\mathbf{y}_{7_y}$ , representing the  $y$  field distribution incident on the photo-detector.
- 

*Step 9* Calculate the signal from the differential amplifier,  $I_{j,i}$ , at the current scan position,  $(j, i)$ , by subtracting the signals from the two photo-detectors, i.e.  $I_{Det1} - I_{Det2}$ .

*Step 10* Repeat *Steps 4 - 9* for each scan position along the sample to generate the response along the current scan line.

*Step 11* Centre the focused field distribution on the next scan line and repeat *Steps 4-10* for each scan line to generate a two dimensional matrix,  $I$ , representing the image of the two-dimensional object generated by the Type 1 differential detector MO scanning microscope.

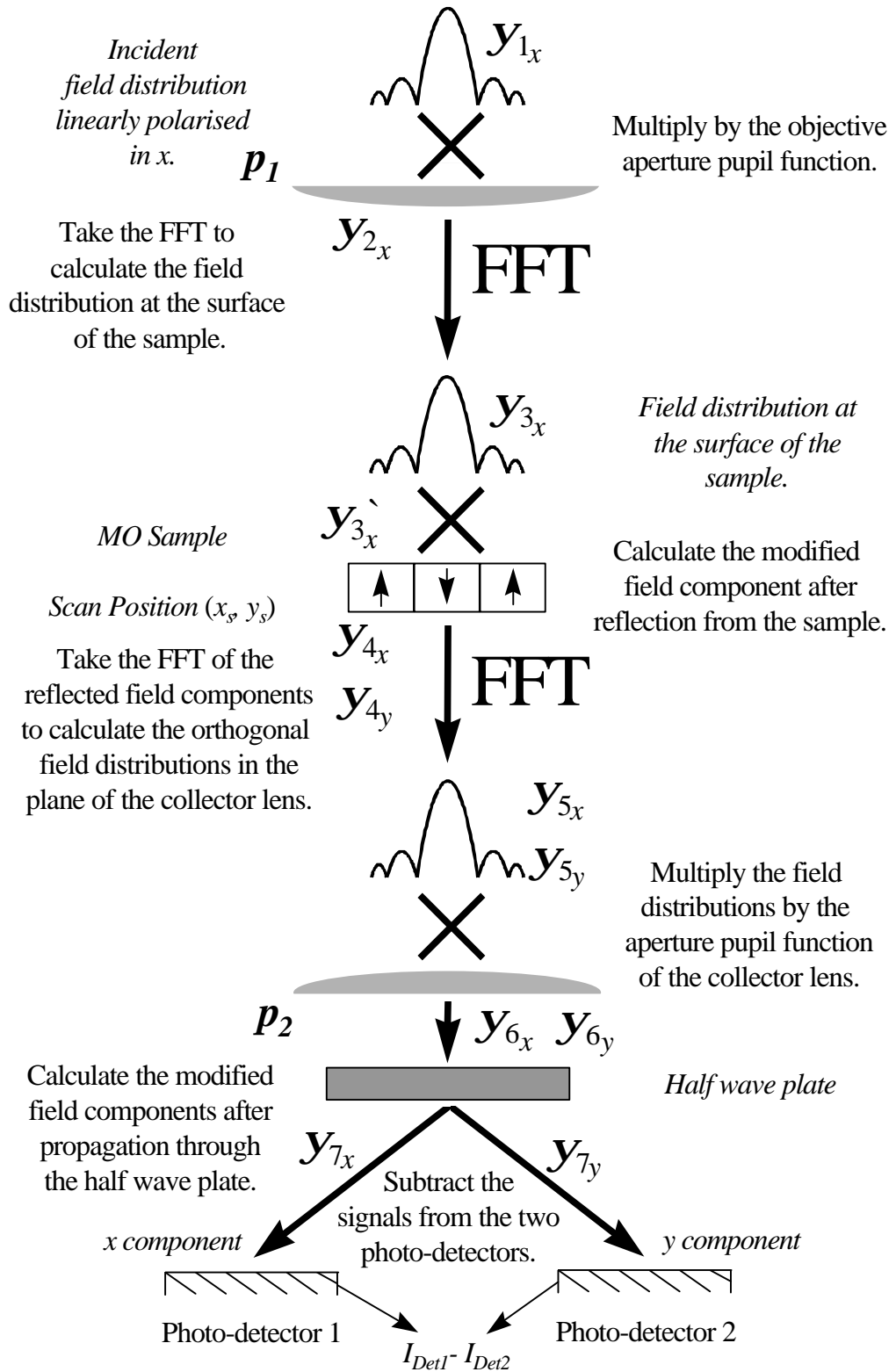


**Figure 5.13 :** The signal generation process in the Type 1 differential detector MO system using the direct calculation approach.





Set  $j = 0$ .                      Current scan line  $j$ )

*Step 4*                      FOR  $y = 1, 2, \dots, fdim$   
                                     FOR  $x = 1, 2, \dots, fdim$   
                                     Set  
 $\mathbf{y}_{4_x}(y + (mdim - fdim) / 2, x + (mdim - fdim) / 2) =$   
 $\mathbf{y}_{3_x}'(y, x) \times r((y + j), (x + i));$   
 $\mathbf{y}_{4_y}(y + (mdim - fdim) / 2, x + (mdim - fdim) / 2) = \mathbf{y}_{3_x}'(y, x)$   
 $\times r((y + j), (x + i)) \times k((y + j), (x + i)) \times \mathbf{f}((y + j), (x + i));$   
                                     END;

END.

*Step 5*                      Set  $\mathbf{y}_{5_x} =$  Fast Fourier Transform ( $\mathbf{y}_{4_x}$ );<sup>#1</sup>  
                                     Set  $\mathbf{y}_{5_y} =$  Fast Fourier Transform ( $\mathbf{y}_{4_y}$ ).<sup>#1</sup>

*Step 6*                      FOR  $y = 1, 2, \dots, adim$   
                                     FOR  $x = 1, 2, \dots, adim$   
                                     Set  
 $\mathbf{y}_{6_x}(y + (mdim - adim) / 2, x + (mdim - adim) / 2) =$   
 $\mathbf{y}_{5_x}(y + (mdim - adim) / 2, x + (mdim - adim) / 2) \times p_c(y, x);$   
 $\mathbf{y}_{6_y}(y + (mdim - adim) / 2, x + (mdim - adim) / 2) =$   
 $\mathbf{y}_{5_y}(y + (mdim - adim) / 2, x + (mdim - adim) / 2) \times p_c(y, x);$   
                                     END;

END.

*Step 7*                      FOR  $y = 1, 2, \dots, mdim$   
                                     FOR  $x = 1, 2, \dots, mdim$   
                                     Set  $\mathbf{y}_{7_x}(y, x) = \mathbf{y}_{6_x}(y, x) \cos 2\mathbf{q} + \mathbf{y}_{6_y}(y, x) \sin 2\mathbf{q};$   
                                     Set  $\mathbf{y}_{7_y}(y, x) = -\mathbf{y}_{6_y}(y, x) \sin 2\mathbf{q} + \mathbf{y}_{6_x}(y, x) \cos 2\mathbf{q};$   
                                     END;

END.

*Step 8*                      Set  $I_{Det1}(j, i) = \sum_{y=1}^{y=mdim} \sum_{x=1}^{x=mdim} |\mathbf{y}_{7_x}(y, x)|^2;$   
                                     Set  $I_{Det2}(j, i) = \sum_{y=1}^{y=mdim} \sum_{x=1}^{x=mdim} |\mathbf{y}_{7_y}(y, x)|^2;$   
                                     Set  $i = i + 1$ <sup>#3</sup>.                      (Increment the scan position)

*Step 9*                      Set  $I(j, i) = I_{Det1}(j, i) - I_{Det2}(j, i).$

*Step 10*                     WHILE  $i < (odim - fdim)$  DO Steps 4-9.

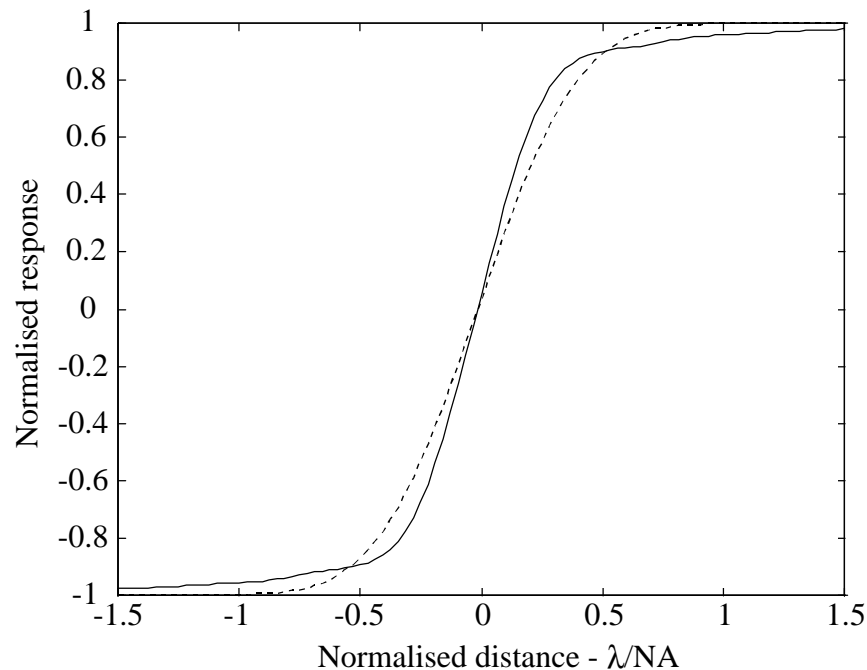
*Step 11*                     Set  $j = j + 1;$                       (Increment the scan line)  
                                     WHILE  $j < (odim - fdim)$  DO Steps 4-10;  
                                     STOP.

<sup>#1</sup> Fast Fourier Transform algorithm is described in reference 68.

The one-dimensional response may be generated as described for the Type 1 reflectance scanning microscope.

### Step response

Figure 5.14 illustrates the step response the Type 1 differential detector MO scanning microscope, generated using the algorithm presented above. The responses of Fig. 5.14 were generated using the MO object of Fig. 5.8 with clear, aberration free, circular apertures under uniform and Gaussian ( $w_{e^{-2}}=a/2$ ) incident illumination, for a half wave plate angle of  $22.5^\circ$  to the plane of incident polarisation (ideal case).



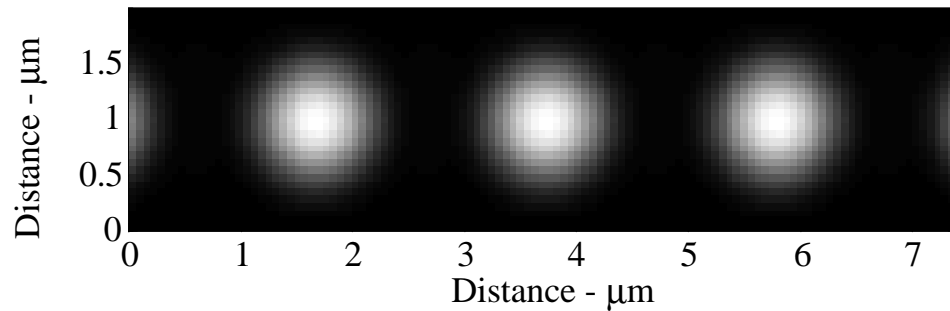
**Figure 5.14** : *The Kerr step response of the Type 1 differential detector MO system for clear, aberration free, circular apertures of equal diameter under uniform (solid line) and Gaussian ( $w_{e^{-2}} = a/2$ ) (dashed line) incident illumination, for an half wave plate orientation of  $\mathbf{q}=22.5^\circ$  to plane of incident polarisation,  $x$ , generated using the direct calculation approach.*

Figure 5.14 illustrates that the response of the Type 1 differential detector MO scanning microscope is very different to that of the single detector configuration with analyser set to extinction, Fig. 5.9. Due to the half wave plate, polarising beamsplitter

and differential detector arrangement, the Type 1 differential detector MO scanning microscope is able to distinguish the polarity of the rotation, as well as the magnitude of the rotation. Figure 5.14 clearly illustrates the form of the incident illumination affects the response of the scanning microscope, a result that was illustrated when investigating the reflectance system, sec. 5.1. However, unlike the Type 1 reflectance scanning microscope, the MO response is symmetrical about the centre of the edge.

### Two-dimensional imaging

Figure 5.15 illustrates the image of the bits of Fig 5.10 for the Type 1 differential detector case. The image was generated with clear, aberration free, circular apertures of equal diameter under uniform incident illumination.



**Figure 5.15 :** *Image of the MO bits of Fig 5.10, using the Type 1 differential detector MO scanning microscope generated using the direct calculation approach.*

Figure 5.16 shows the effects on the signal amplitude when scanning the focused beam along a track at varying distances from the centre of the track, and clearly illustrates the effects of tracking error in optical storage systems.

Figure 5.16 indicates that for a tracking error of  $0.75\mu\text{m}$ , the signal magnitude has decreased to 5% of the maximum (along the track centre).

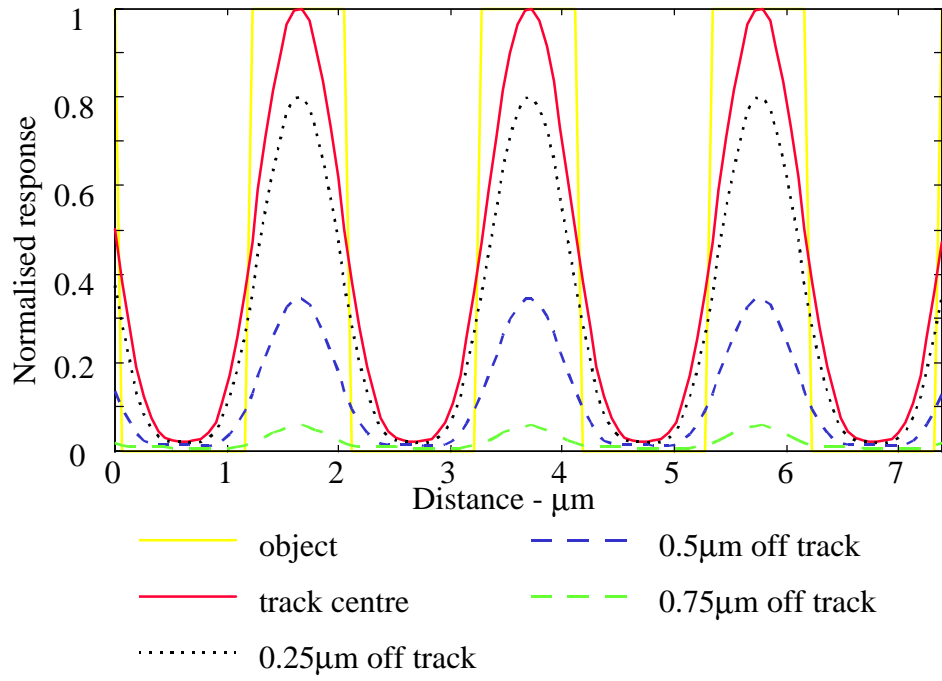


**Figure 5.16 :** *Plots of signal profile at varying distances from the track centre for the two-dimensional image illustrated in Fig. 5.15.*